Clim. Past Discuss., 6, 1229–1265, 2010
www.clim-past-discuss.net/6/1229/2010/
doi:10.5194/cpd-6-1229-2010

Climate of the Past Discussions

Sea-surface salinity variations in the Northern Caribbean Sea across the mid-Pleistocene transition

S. Sepulcre, L. Vidal, K. Tachikawa, F. Rostek, and E. Bard

CEREGE, UMR6635, Université Aix-Marseille, CNRS, Collège de France, IRD, Europôle de l'Arbois, BP80, 13545 Aix-en-Provence, France

Received: 4 June 2010 – Accepted: 14 June 2010 – Published: 29 June 2010

Correspondence to: S. Sepulcre (sepulcre@cerege.fr)

Published by Copernicus Publications on behalf of the European Geosciences Union.

Abstract

This study aimed at documenting climate changes in tropical area in response to the Mid-Pleistocene Transition (MPT) by reconstructing past hydrologic variations in the Northern Caribbean Sea and its influence on the stability of the Atlantic Meridional Overturning Circulation (AMOC) during the last 940 kyr. Using core MD03-2628, we estimated past changes in sea surface salinity (SSS) using $\Delta\delta^{18}O$, the difference between the modern and the past $\delta^{18}O$ of seawater (obtained by combining alkenone thermometer data with the $\delta^{18}O$ of the planktonic *foraminifera Globigerinoides ruber* (white) and corrected for ice-sheet volume effects). Today, the lowest SSS values in the studied area are associated with the northernmost location of the Inter-Tropical Convergence Zone (ITCZ). The $\Delta\delta^{18}O$ record exhibits glacial/interglacial cyclicity with higher values during all glacial periods spanning the last 940 kyr, indicating increased SSS. At a longer timescale, the $\Delta\delta^{18}O$ exhibits a shift toward lower values for interglacial periods during the last 450 kyr, when compared to interglacial stages older than 650 kyr. A rise in SSS during glacial stages may be related to the southernmost location of the ITCZ, which is induced by a steeper interhemispheric temperature gradient and associated with reduced northward cross equatorial oceanic transport. Therefore, the results suggest a permanent link between the tropical salinity budget and the AMOC during the last 940 kyr. Following the MPT, lower salinities during the last five interglacial stages indicate a northernmost ITCZ location, forced by changes in the interhemispheric temperature gradient that is associated with the poleward position of Southern Oceanic Fronts that amplified the transport of heat and moisture to the North Atlantic. These processes may have contributed to amplification of the climate cycles that followed the MPT.

1 Introduction

The Mid-Pleistocene Transition (MPT) corresponds to the period that lead to the emergence of low-frequency, quasi-periodic climate cycles of asymmetrical shape and 100-kyr length, and that varied between 1.5 Myr to 650 kyr depending upon the paleoclimatic archive utilized (e.g., Head and Gibbard, 2005). In the absence of a marked change in insolation forcing (e.g., Maslin and Ridgwell, 2005), several hypotheses have been explored in order to explain this transition such as long-term changes the atmospheric CO_2 (Clark et al., 2006), changes in the ice-sheet bedrock or the so-called "regolith hypothesis" (Clark and Pollard, 1998), or changes in ice-sheets dynamics (e.g., Berger et al., 1999; Tziperman and Gildor, 2003; Bintanja and van de Wal, 2008) leading to the progressive synchronization of the Northern Hemisphere and the Antarctic ice-sheets (Raymo et al., 2006). The latter hypothesis implies a series of internal feedbacks such as changes in deep-water circulation (McClymont et al., 2008) or in the oceanic carbon pool (Raymo et al., 1990, 1997; Mix et al., 1995; Schmieder et al., 2000; Hoogakker et al., 2006). Other studies have invoked the role of the tropics (McClymont and Rosell-Melé, 2005; Liu et al., 2008) or the Southern Hemisphere (Raymo et al., 2006; Schulz and Zeebe, 2006; Köhler and Bintanja, 2008). However, no theory has supplanted another and no real consensus has been adopted to explain the causes for the MPT (e.g., Raymo and Huybers, 2008). In particular, the relationships between low and high latitudes during this time period remain un-explored (Rutherford and D'Hondt, 2000). In this work, we sought to document the impact of global climate changes associated with the MPT in the tropical area using a marine sediment core obtained from the Northern Caribbean Sea. The Tropical Atlantic is a key area in the modern climate system due to its role in the stability of the Atlantic Meridional Overturning Circulation (AMOC) which transports warm and salty waters from low latitudes into the North Atlantic. The efficiency of the AMOC may have a major impact on global climate change, particularly in Northern Atlantic areas as suggested by model experiments and paleoclimatic data (e.g., Rahmstorf, 2002). Specifically, model simulations

CPD
6, 1229–1265, 2010

suggest that the strength of the AMOC is more sensitive to changes in the Atlantic salt budget than to variations in sea-surface temperature (SST) and therefore point to the importance of reconstructing past changes in the low latitude hydrologic cycles (Rahmstorf et al., 2005; Rahmstorf, 2006). Under modern conditions, the Atlantic salt budget is determined by a combination of local and regional processes partly linked to tropical climate dynamic, such as the following:

1. The seasonal migration of the inter tropical convergence zone (ITCZ) which impacts the local salt budget in the Tropical Atlantic through direct freshwater inputs via precipitation as well as by the amount of freshwater exported toward the Pacific (Broecker et al., 1990; Zaucker and Broecker, 1992);

2. The duration and amplitude of the northward shift of the ITCZ. The northern ITCZ location is associated with the enhanced cross-equatorial transport of salt and heat into the North Atlantic (e.g., Dahl et al., 2005). The effect of ITCZ migration is clearly observed for meridional heat transport in the oceans, showing an inter-hemispheric asymmetrical behavior for the Atlantic basin (Trenberth and Caron, 2001);

3. A remote control of the salt amount exported from the Indian Ocean to the Tropical Atlantic via the South Atlantic through the "Agulhas leakage" (AL) under modern and past conditions (Gordon, 1996; Peeters et al., 2004; Biastoch et al., 2008). The relationships between Tropical Atlantic hydrology, the AMOC, and climate changes have been determined through estimations of the salt budget at low latitudes during rapid climate change (Rühlemann et al., 1999; Schmidt et al., 2004), during glacial/interglacial climate transitions (Dürkoop et al., 1997), and on long time scales (Haug and Tiedemann, 1998; Haug et al., 2001), as well as through modelling studies (Wan et al., 2010).

In this study, we examined climate changes associated with the MPT in the tropics by estimating past variations in hydrologic conditions in the Northern Caribbean

CPD
6, 1229–1265, 2010

Sea and related changes in the AMOC. Here, we discuss the variations of past sea-surface salinity (SSS) related to the ITCZ location, and estimate past SSS at the core site through the δ^{18}O of seawater, by combining oxygen isotopic measurements obtained from the surface-dwelling planktonic foraminifer *Globigerinoides ruber* (white) with SSTs obtained from the alkenone unsaturation index ($U_{37}^{K'}$) analysis. We have corrected the δ^{18}O of seawater for ice-sheet volume effects and have calculated the $\Delta\delta^{18}$O as the difference between the modern and past δ^{18}O for seawater. The major trends observed in the $\Delta\delta^{18}$O record were that a marked glacial/interglacial pattern spanned the entire record and that a shift toward decreased SSS during interglacials occurred for the last 450 kyr compared to the previous time interval (650–940 kyr). At the glacial/interglacial timescale, the core MD03-2628 results emphasize the existing link between the ITCZ and the AMOC over the past 940 kyr. The results obtained for interglacial stages for the last 450 kyr allowed us to discuss the causes and consequences of ITCZ migration following the MPT, and the possible relationships between changes in oceanic and atmospheric northward heat transfer associated with ITCZ migration.

2 Modern climate and hydrologic parameters

Core MD03-2628 was retrieved in the Walton Basin (17°21.26′ N, 77°42.45′ W, 846 m water depth, Fig. 1) during the IMAGES MD132 expedition, aboard R.V. *Marion Dufresne* in 2003. The Walton Basin is located in the northeastern portion of the Nicaragua Rise, which separates the Colombian Basin from the Cayman Basin (Fig. 1a). The Walton Basin consists of a deep seaway between the Jamaican shelf and the Pedro Bank, with water depths ranging between 200 and 2000 m (Fig. 1b). Modern climate and oceanographic data near the core MD03-2628 location (Fig. 1b) were extracted from the DASILVA dataset (precipitation and evaporation rates were obtained at 17.5° N, 77.5° W, da Silva et al., 1994), the NOAA data center (atmospheric temperature at Montego Bay, 18.47° N, 77.99° W, Jamaica), and the LEVITUS (1994) dataset (at 17.5° N, 77.5° W).

CPD
6, 1229–1265, 2010

2.1 Climatology and hydrologic parameters

The climate in the Caribbean Sea is typically tropical without a pronounced cooling season (Fig. 2a). A maximum easterly zonal wind at 925 hPa in the Caribbean region is called the Caribbean Low-Level Jet (CLLJ). The CLLJ is at its maximum in winter (Fig. 1a), when the atmospheric temperature gradient between the Caribbean zone and the Tropical North Atlantic is large and the ITCZ is further South (Wang and Lee, 2007). The summer wet period extends from May to November and can be divided in two time intervals (Fig. 2b, Taylor et al., 2002). From May to July, precipitation reaches 90 mm/month and from August to November, during the hurricane season, values increase to 130 mm/month as a result of ITCZ positioning (Figs. 1a, 2b, and 3c; see Sect. 2.2 for details). Evaporation rates (Fig. 2c) exhibit small seasonal variations, with maximum values occurring during winter (183 mm/month in December) and minimal values occurring during spring (120 mm/month in May). Seasonal changes may be related to the strength of the CLLJ (see above).

Near the core MD03-2628 location, hydrographic conditions indicate that SST-monthly variations are limited, within a range of 26.5 to 29 °C, with a trend of high and low values during boreal summer and winter, respectively (Fig. 2e). Monthly surface water salinity (SSS) ranges between 35.6 and 36.1 p.s.u. (Fig. 2d) and is mainly controlled by seasonnal ITCZ migration and freshwater advection (see Sect. 2.2 for details) (Fig. 1a). SSS minimum values from September to December are linked with the northern location of the ITCZ position during September and a "late" contribution of the freshwater supply from the Orinoco River (see below) whereas SSS maximum values are reported in July. No clear relationship appears to exist between the evaporation rate and SSS at the core MD03-2628 location (Fig. 2c, d).

2.2 Salinity variability and surface-water circulation

Caribbean Surface Water (0–50 m) flows from the southeast toward the northwest within the Caribbean Current (Fig. 1a) (Wüst, 1964; Tomczak and Godfrey, 2003), and

CPD
6, 1229–1265, 2010

results from the mixing of South Atlantic Water from the Guyana Current and Equatorial water from the North Equatorial Current (Fig. 1a) (Schmitz and Richardson, 1991).

Seasonal SSS variations are determined by the position of the ITCZ through both direct inputs of freshwater from local precipitation and the advection of low SSS water by surface currents. In March, the ITCZ reaches its southernmost location and provides freshwater to the Amazon Basin (Fig. 3a). The freshwater supply to the studied area is limited and SSS values are 35.9 p.s.u. (Figs. 2d and 3e). In June, the ITCZ is located further north above the Orinoco Basin (Fig. 3b). During that time, maximum discharge of the Amazon River is observed (Fig. 3f, Morrisson and Nowlin, 1982; Müller-Karger et al., 1988; Hernandez-Guerra and Joyce, 2000; Hellweger and Gordon, 2002; Chérubin and Richardson, 2007). However, the low SSS waters that are transported northwards through the Guyana Current do not reach the Northern Caribbean Sea (Figs. 2d, 3f,g). As a result, the SSS value at the site location is high (36.1 p.s.u., Figs. 2d and 3f). Migration of the ITCZ to its northernmost location in September results in high precipitation rates over the studied area (Figs. 2b and 3c) and SSS values decrease to 35.8 p.s.u. (Figs. 2d and 3g). Freshwaters originating from the Orinoco River flow westward in the Caribbean Sea (Fig. 3g, Chérubin and Richardson, 2007). In December, the ITCZ moves southward (Fig. 3d) and Orinoco freshwaters reach the study area causing a decrease in SSS to a level of 35.7 p.s.u. (Chérubin and Richardson, 2007) (Figs. 2d and 3h).

Under modern conditions, SSS seasonnal variability at the core site is best explained by the northward position of the ITCZ during boreal summer as a result of in situ freshwater input by precipitation during September and a "delayed" advection of low SSS waters during late summer (September to November) from the Orinocco River which freshwater supply occurs in June. Therefore, in the following, we associate low SSS values with the northern location of the ITCZ.

CPD
6, 1229–1265, 2010

2.3 Oceanic intermediate and deep-water circulation

Below surface waters, Subtropical UnderWater (SUW) lies between 50 and 300 m in the Caribbean Sea. The SUW water mass originates in the Sargasso Sea and is characterized by a salinity maximum of 36.7 p.s.u. (Morrison and Nowlin, 1982). Antarctic Intermediate Water (AAIW) is found at intermediate water depths (300–1000 m) and mixed with underlying North Atlantic Deep Water (NADW) (Wüst, 1964; Fratantoni et al., 1997; Tomczak and Godfrey, 2003). Deeper than 1000 m, the Caribbean Sea is filled with NADW that has a salinity of approximately 35 p.s.u. (Wüst, 1964; Fratantoni et al., 1997; Tomczak and Godfrey, 2003).

2.4 *Globigerinoides ruber* and coccolithophorid distribution in the water column

Even if the Caribbean Sea is an oligotrophic area, primary productivity (PP) shows seasonal variability. Maximum PP occurs between February and April when nutrients are carried to the Northern Caribbean Sea either from upwelling activity that is created by the CLLJ (Müller-Karger et al., 1988; Hu et al., 2004) in the Southern portion of the Caribbean Sea, or by river plumes that are carried by the Guyana Current (Martinez et al., 2007 and references therein).

The planktonic foraminifer specie *G. ruber* inhabits the upper portion of the water column, between 0 and 20 m (Schmuker and Schiebel, 2002), with corresponding temperature and salinity averaged values of 27 °C and 35.9 p.s.u., respectively (February to April period, Fig. 2d,e).

Coccolithophorids that produce C_{37} alkenone molecules occupy the entire photic zone of the Caribbean Sea, corresponding roughly to the depth of the nutricline (Kameo et al., 2004). In the Northern Caribbean Sea, the nutricline fits within the limit of surface waters and the SUW (i.e. the first 50 m of the water column). Average values of temperature and salinity during the February to April period in the first 50 m are 26.8 °C

CPD
6, 1229–1265, 2010
Sea-surface salinity changes in the Caribbean Sea
S. Sepulcre et al.

(± 0.12 °C, 1σ, where σ is the standard deviation) and 35.9 p.s.u. (± 0.02 p.s.u., 1σ), and can be considered constant for the first 50 m of the water column.

3 Methods

Core MD03-2828 was sampled at every 20 cm interval for the $\delta^{18}O$ analysis and for the $U^{K'}_{37}$ determination. Samples for $\delta^{18}O$ measurements were wet-sieved for the <63 µm, 63–150 µm, and >150 µm fractions and dried in an oven at 50 °C. *G. ruber* (250–355 µm) was hand-picked from the >150 µm fraction. Samples for the alkenone analysis were freeze-dried and ground in a mortar. All of the preparations and instrumental measurements were carried out at CEREGE.

$\delta^{18}O$ measurements were performed on five to ten individuals of *G. ruber* using a Finnigan Delta Advantage mass spectrometer directly coupled to an automatic carbonate preparation device calibrated to the international scale (Vienna Pee Dee Belemnite VPDB). Analytical precision of the method was controlled with the regular standard analyses of NBS19 and was better than 0.04‰ for $\delta^{18}O_{VPDB}$ (1σ; n=169).

The analytical procedure and the extraction method for the C_{37} alkenone measurements are fully described in Sonzogni et al. (1997). The quality of the measurements carried out at CEREGE was confirmed by an international intercalibration study (Rosell-Melé et al., 2001). The analytical accuracy was approximately 0.01 (1σ). SSTs were calculated with the $U^{K'}_{37}$ index using the calibration of Sonzogni et al. (1997) for the 24–29 °C temperature range. The uncertainty in the reconstruction was 0.7 °C. The calibration is more suitable to high SST values rather than global calibrations, such as those of Conte et al. (2006).

CPD
6, 1229–1265, 2010

4 Results

4.1 Stable isotopic record

The chronology in core MD03-2628 is based on the *G. ruber* $\delta^{18}O$ record (Fig. 4a) and paleomagnetic measurements and has been fully described elsewhere (Sepulcre et al., 2009). Briefly, the age model was obtained using a correlation of the $\delta^{18}O$ record with a reference record (Lisiecki and Raymo, 2005) using the software "Analyseries" (Paillard et al., 1996). The isotopic correlation was supported by the identification of paleomagnetic events in core MD03-2628, such as the Delta (~685 kyr), the Kamikatsura (~900 kyr), the Santa Rosa (~940 kyr), and the Bruhnes-Matuyama reversal (~780 kyr). The core MD03-2628 record spans the last 940 kyr, up to MIS 24 (Fig. 4a). The average sedimentation rates for interglacial and glacial periods are 4 and 2 cm/kyr, respectively, with a corresponding time-resolution of 5 and 10 kyr.

$\delta^{18}O$ values of *G. ruber* ranged from −2.2 (Holocene) to 1.2‰ (MIS 16) (Fig. 4a). The results are in good agreement with previous planktonic $\delta^{18}O$ records from the Caribbean Sea spanning the last 350 kyr (Wolff et al., 1998; Schmidt et al., 2004, 2006). Except for MIS 16, the $\delta^{18}O$ values for glacials are nearly constant at approximately 0–0.4‰ for the overall record. From 940 to 650 kyr, glacial-interglacial amplitudes of $\delta^{18}O$ variations through glacial Terminations were approximately 1‰, with values for interglacials ranging between −1.4 and −0.7‰ (Figs. 4a and 5). Between 650 and 450 kyr (from MIS 16 to MIS 13), we observed a very high value for MIS 16 out of the range for the other glacial $\delta^{18}O$ values recorded and a $\delta^{18}O$ value for MIS 14 as high as a cold event during MIS 15 (Figs. 4a and 5). Glacial-interglacial amplitudes across glacial Terminations from 450 kyr to the core top increased to approximately 2‰ as compared to the oldest time interval. The change in amplitude is due to a shift in interglacial stage values toward lower $\delta^{18}O$, ranging from −2.2 to −1.4‰ (Figs. 4a and 5).

The 650–450 kyr time-interval corresponds to a transition period between the end of the MPT at 650 kyr and the setting of climate cycles of asymmetrical shape, a 100-kyr

CPD
6, 1229–1265, 2010

length and a higher glacial/interglacial amplitude for the last 450 kyr (e.g., Tzedakis et al., 2009; Yin and Berger, 2010). Therefore, in the following we decided to compare the time-interval corresponding to the end of the MPT from 940 to 650 kyr with the period spanning the last 450 kyr, when the δ^{18}O record clearly exhibited a change in climate cycles, especially for the glacial/interglacial amplitude during glacial Terminations (Figs. 4a and 5).

The core top value for δ^{18}O of *G. ruber* was −2‰, very close to the expected value (−2.3‰) obtained when using the equation of Mulitza et al. (2003) and modern hydrologic data ($\delta^{18}O_{seawater}$=1.01‰ from the Global Seawater δ^{18}O Database (Schmidt et al., 1999) and mean annual SST=27.8 °C at the core location). The Mulitza et al. (2003) equation provided a result that is in better agreement with the measured δ^{18}O than the Bemis et al. (1998) equation. The core top δ^{18}O value is close to the calculated value even when we considered the possible shifts between modern and fossil *G. ruber* from Holocene samples (Waelbroeck et al., 2005). In the following, we used the equation of Mulitza et al. (2003) to calculate the δ^{18}O record of seawater.

4.2 Paleosea-surface temperatures

The SST record of core MD03-2628 exhibited well-defined glacial-interglacial cyclicity, with lower values during glacials (Fig. 4b). The core top SST showed a value of 27.7 °C, in good agreement with modern annual SST (Fig. 2e). SST values ranged from a minimum value of 24.8 °C (MIS 22) to a maximum value of 28.1 °C (MIS 15). Interglacial and glacial stages had an average SST of 27.3 °C (± 0.07 °C, $1\sigma_m$, with $\sigma_m=\frac{\sigma}{\sqrt{n}}$ and n=69) and 26.5 °C (± 0.14 °C, $1\sigma_m$, n=36), respectively. The average amplitude of the glacial-interglacial change was approximately 1.9 °C (± 0.17 °C, $1\sigma_m$, n=11), with values ranging from 0.78 to 2.8 °C (Terminations VI and X, respectively). No long-trend was observed in the SST record.

Since, here, we present the first alkenone-based SST reconstruction available for the Caribbean Sea, our data was compared with previous SST records from the same

CPD
6, 1229–1265, 2010

area obtained from micropaleontological assemblages (Hüls and Zahn, 2000; Schmidt et al., 2006; Martinez et al., 2007) and foraminiferal Mg/Ca (Hastings et al., 1998; Schmidt et al., 2004, 2006) (ODP core 999A, Figs. 1a and 6). The SST difference through Termination I was well-documented, showing a glacial to interglacial change ranging from 1 to 4 °C (Fig. 6b,c). Thus, the value of approximately 2 °C determined in core MD03-2628 (Fig. 6a) is in the range of previous reconstitutions. For the last 350 kyr, all of the SST records exhibited a glacial/interglacial pattern with a similar amplitude for glacial Terminations except for the MIS5e Mg/Ca-SSTs (showing values up to 29.5 °C) and MIS3 micropaleontological-SSTs (values as low as 23 °C; Fig. 6). SST variability in core MD03-2628 was less pronounced than in the Mg/Ca-SST record, in particular during interglacial periods and during glacial Termination II. On the other hand, SSTs from core MD03-2628 displayed a larger amplitude during Termination IV than Mg/Ca-SSTs from core ODP 999 (Fig. 6b). However, for the later record, a partial dissolution of the foraminiferal tests affecting the SST reconstruction was seen from 465 to 360 kyr (Schmidt et al., 2006). In general, lower variability in core MD03-2628 SST reconstructions could be related to the lower temporal resolution of the record. Part of the observed discrepancies may also be related to the different core sites, and in particular the nearly permanent location inside the Atlantic Warm Pool for core ODP 999A, unlike core MD03-2628 (for a complete discussion, see Ziegler et al., 2008). Therefore, even when taking into account the few differences between available SST reconstructions, general agreement was found between the alkenone-SST record in core MD03-2628 and other SST records, supporting the application of alkenone-SST to estimations of paleohydrological variability in the Northern Caribbean Sea.

4.3 The calculation of local surface δ^{18}O variability

By combining the δ^{18}O of *G. ruber* and the alkenone-SST records of core MD03-2628, we estimated the δ^{18}O of seawater at the core location (Fig. 7a). Glacial-interglacial variability was well-expressed using the past δ^{18}O of seawater, with values ranging from 1.05 to 4.12‰ and with a trend of higher δ^{18}O during glacials. Glacial values

CPD
6, 1229–1265, 2010

were nearly constant for the 940–650 kyr time interval when compared to the 450–0 kyr period, with values of 3.08 ± 0.06‰ ($1\sigma_m, n$=12) and 2.97± 0.07‰ ($1\sigma_m, n$=15), respectively. Interglacial stages displayed the same pattern as the δ^{18}O of *G. ruber*, with lower values of 0.61‰ (± 0.07, $1\sigma_{\mathrm{sum}}, \sigma_{\mathrm{sum}}=\sqrt{\sigma_1^2+\sigma_2^2}$) for the last 450 kyr (1.7‰ ± 0.05, $1\sigma_m, n$=37) as compared to the 940–650 kyr time interval (2.3‰ ± 0.04, $1\sigma_m, n$=24). Taking into account the uncertainty of the SST reconstruction (± 0.7 °C) lead to a 0.23‰ error for the calculation of the past δ^{18}O of seawater, a value that is lower than the difference of 0.61‰ observed for interglacial stages from 940–650 kyr and from 450–0 kyr, and the average glacial-interglacial amplitude of 1.46‰ (± 0.17, $1\sigma_m, n$=11). In order to better document the glacial-interglacial pattern as well as the long-term trend in the Northern Caribbean Sea, we corrected the MD03-2628 δ^{18}O of seawater using global ice volume changes, as described below.

For the last 430 kyr, two reconstructions of the ice volume effect (IVE) obtained from Waelbroeck et al. (2002) and Bintanja and van de Wal (2008) were used (Fig. 7b). In general, good agreement was observed between the IVE curves for the last 430 kyr (Fig. 7b). The global δ^{18}O of seawater was finally subtracted from the calculated local δ^{18}O of seawater at the core MD03-2628 location. For easier comparison, here we present the difference between the δ^{18}O of seawater in the past and the δ^{18}O of modern seawater (1.01‰), which is indicated as $\Delta\delta^{18}$O (Fig. 7c). To fully account for the variability induced by the IVE correction, we used the average δ^{18}O of seawater from both the IVE reconstructions for the time interval from 0–430 kyr (Fig. 7b). We only used the Bintanja and van de Wal (2008) δ^{18}O of the seawater reconstruction for the 940–430 kyr time period (Fig. 7b).

Conversion of the δ^{18}O of seawater into paleo-SSS values may be uncertain due to a lack of information regarding the temporal evolution for the δ^{18}O of the seawater/SSS relationship (that is the $\delta^{18}O_{\mathrm{seawater}}=0.263(\pm0.06)\times S-8.57(\pm1.99)$ at the core site if we consider calibrations from the Caribbean Sea and the Tropical Atlantic of Watanabe et al., 2001, Steph et al., 2006, and Regenberg et al., 2009). Therefore, we decided to discuss the change in $\Delta\delta^{18}$O as a proxy for variations in SSS relative to modern conditions (Fig. 7c). The $\Delta\delta^{18}$O record exhibited a glacial/interglacial pattern with high and low values during glacial and interglacial stages, respectively, for the last 940 kyr (Fig. 7c). Average interglacial values were 0.95‰ (±0.05‰, $1\sigma_m, n=24$) for the last 450 kyr, and 0.5‰ (±0.05‰, $1\sigma_m, n=37$) for the 940–650 kyr time-interval, resulting in a $\Delta\delta^{18}$O difference between the two periods of 0.45‰ (±0.07‰, $1\sigma_{\mathrm{sum}}$). On the contrary, we observed a trend of nearly constant $\Delta\delta^{18}$O for all of the glacial stages throughout the record, with average values of 1.35‰ (±0.07‰, $1\sigma_m, n=12$) and 1.25‰ (±0.06‰, $1\sigma_m, n=15$) from 940 to 650 kyr and from 450 to 0 kyr, respectively. Hereafter, we refer to an average glacial $\Delta\delta^{18}$O value of 1.3‰ (±0.09‰, $1\sigma_{\mathrm{sum}}$) for both time-intervals.

On glacial-interglacial timescales, variations in the $\Delta\delta^{18}$O from −0.35 to 0.65‰ have been described for the last 130 kyr in the Caribbean Sea (Schmidt et al., 2004). For the same time interval, $\Delta\delta^{18}$O results ranged from −0.02 and 1.5‰. A higher $\Delta\delta^{18}$O amplitude of change in core MD03-2628 may be related to a less pronounced variability in the SST record when compared to previous works, mainly due to the low resolution of core MD03-2628 sampling and a decrease in sedimentation rates during glacial stages (Fig. 6). In spite of the difference in the $\Delta\delta^{18}$O amplitude, the same trend was found in both reconstructions with high values during glacials and low values during interglacials. Additionally, the average glacial/interglacial difference for core MD03-2628 $\Delta\delta^{18}$O resulted in 0.8‰ (±0.1‰, $1\sigma_{\mathrm{sum}}$), in good agreement with the amplitudes of 0.5 and 0.8‰ as determined for the last two glacial Terminations in the Caribbean Sea, respectively (Schmidt et al., 2004), and with a study in the Tropical Atlantic for the last Termination (Wolff et al., 1998).

CPD
6, 1229–1265, 2010

Title Page
Abstract | Introduction
Conclusions | References
Tables | Figures
◂◂ | ▸▸
◂ | ▸
Back | Close
Full Screen / Esc
Printer-friendly Version
Interactive Discussion

5 Discussion

Reconstruction for the regional $\Delta\delta^{18}O$ of seawater in the Northern Caribbean Sea has revealed two major trends – a marked glacial/interglacial pattern spanning the last 940 kyr and a shift toward lower surface water $\Delta\delta^{18}O$ during interglacial stages over the last 450 kyr (Fig. 8a). In both cases the results are interpreted as changes in the salinity budget at the core location. After validating our reconstructions, the climate mechanisms responsible for these hydrologic changes and their implications are discussed according to the following main lines:

1. Processes influencing the ITCZ location on glacial-interglacial timescales. We refer to the evidence for the ITCZ migration in paleoclimatic records and discuss the mechanisms involved based on modeling results. Changes in the cross-equatorial transport of salt and heat into the North Atlantic associated with the ITCZ migration, and their related consequences on the AMOC, are also considered;

2. Using the mechanisms pointed out for the glacial-interglacial timescale, we discuss the possible causes and consequences of an ITCZ migration for interglacial stages spanning the last 450 kyr, following the MPT. We especially explore changes in oceanic and atmospheric heat transfers that may have been associated with ITCZ movement, and examine how these different processes may have contributed to the amplification of the climate cycles after the MPT.

5.1 The validity of $\Delta\delta^{18}O$ reconstructions

5.1.1 Glacial/interglacial $\Delta\delta^{18}O$ changes

The glacial/interglacial pattern for the $\Delta\delta^{18}O$ record in core MD03-2628 is clearly documented for the entire record, except for MIS 20 and 22 (Fig. 8a). Even if the mean $\Delta\delta^{18}O$ value changed over time (see below), glacial/interglacial variations of $\Delta\delta^{18}O$ were maintained for the entire record, suggesting that the surface water salinity in-

CPD
6, 1229–1265, 2010

Sea-surface salinity changes in the Caribbean Sea

S. Sepulcre et al.

crease in the Northern Caribbean Sea during glacial stages was a recurrent feature of the last million years. Similar patterns have previously been described for the last glacial/interglacial cycle in the Caribbean Sea (Schmidt et al., 2004) and in the western Tropical Atlantic for the last 350 kyr (Dürkoop et al., 1997). Under modern conditions, the northern position of the ITCZ during boreal summer modulates the freshwater supply to the studied area and, thus, the SSS variability (see Sect. 2.2). The main process for explaining an increase in SSS at the core site is a southern position for the ITCZ that would prevent direct and indirect freshwater supplies during glacial periods. Evidence for southward displacement have already been determined in other paleoclimatic records from the same area (e.g., Schmidt et al., 2004; Ziegler et al., 2008 and references therein). Additionally, it is generally accepted that glacial stages are associated with a reduced AMOC (Schmidt et al., 2004; Stouffer et al., 2006). Therefore, a reduced cross-equatorial flow would keep salty surface waters at low latitudes rather than transport them to the high latitudes of the Northern Atlantic (Crowley, 1992). Such a feature is found in the core MD03-2628 $\Delta\delta^{18}$O record, which reflects an increase in salinity during glacial periods spanning the last 940 kyr, in good agreement with previous modelling studies and paleoceanographic records from tropical areas (Rühlemann et al., 2004; Dahl et al., 2005) (Fig. 8a).

5.1.2 Long-term $\Delta\delta^{18}$O shifts

The other remarkable feature in the $\Delta\delta^{18}$O record of core MD03-2628 is a shift toward lower values occurring during interglacial stages after 450 kyr (Fig. 8a). This trend in local salinity in the Northern Caribbean Sea is robust and is not an artifact produced by the SST reconstruction (Fig. 6) and/or by the global oceanic δ^{18}O (Fig. 7). The SST record in core MD03-2628 does not show any shift between 650 kyr and 450 kyr (Fig. 6b), a feature that is supported by other tropical SST records for the last million years (even if other areas are controlled by different climate processes) (de Garidel-Thoron, 2007; Liu et al., 2008). We have shown that the trend observed in the $\Delta\delta^{18}$O record already exists in the seawater δ^{18}O record reconstructed by only correcting the

CPD
6, 1229–1265, 2010

$\delta^{18}O$ of *G. ruber* for SST without considering the global mean oceanic $\delta^{18}O$ (Fig. 7a). The comparison between core MD03-2628 $\delta^{18}O$ results and other planktonic records supports the fact that the observed trend is related to Caribbean water hydrology. The *Globigerinoides sacculifer* $\delta^{18}O$ record at site ODP 847 in the Eastern Equatorial Pacific (Fig. 1a, Farrell et al., 1995) does show constant mean values for the last million years (Fig. 8b). On the other hand, the *G. sacculifer* $\delta^{18}O$ record from core DSDP 502 obtained from the Caribbean Sea (Figs. 1a and 8b) also shows a significant difference (of approximately 0.4‰) in mean $\delta^{18}O$ values between the late and early Quaternary (Prell, 1982).

Therefore, we suggest that the observed shift in the $\Delta\delta^{18}O$ of core MD03-2628 reflects changes in the regional salinity of the Caribbean Sea mainly during interglacial stages (Fig. 8a). Northerly migration of the ITCZ during interglacials from the last 450 kyr (compared to the period before 650 kyr) can explain these local hydrologic changes. A northward position would bring more freshwater to the site and cause a salinity decrease during interglacials as observed during modern late summer conditions (Figs. 2 and 3).

5.2 Mechanisms for ITCZ migration and links with the AMOC

The processes responsible for the ITCZ migration at glacial-interglacial timescales can be inferred from both modern conditions and modelling results. The modern seasonal migration of the ITCZ is influenced by the interhemipheric temperature gradient, with a relatively warm Northern Hemisphere compared to the Southern Hemisphere; this north-south asymmetry implies that the ITCZ occupies most months of the years the relatively warm Northern Hemisphere (e.g., Chiang et al., 2002, 2003).

As mentioned previously by several authors (Chiang et al., 2003; Broccoli et al., 2006; Stouffer et al., 2006), an interhemispheric temperature contrast was initiated during periods of reduced AMOC and played an important role in ITCZ displacement in the past on a glacial/interglacial timescale. A recent study focused on simulations of the last glacial maximum. Special emphasis on the ITCZ has shown that a southward shift of the ITCZ resulting from an increased equator to pole temperature gradient in the Northern Hemisphere associated with glacial boundary conditions is a robust feature, since it has been observed in several model outputs (Braconnot et al., 2007). The associated oceanic response in the Tropical Atlantic is a warming of thermocline waters that results from a decreased strength of the northward flowing current in surface and thermocline waters (Rühlemann et al., 2004; Dahl et al., 2005). Warm and salty waters stay in the tropics without being exported to the north (Dahl et al., 2005; Wan et al., 2010).

The interesting feature is that the ITCZ migration, related to a change in the inter-hemispheric temperature gradient due to a reduced AMOC, has been mentioned for different timescales corresponding to different modes of climate variability and thermohaline circulation (Rahmstorf, 2000; Stouffer et al., 2006; Wan et al., 2010); glacial stages (Schmidt et al., 2004; Dürkoop et al., 1997; Mix et al., 1986; Ziegler et al., 2008); and during rapid climate changes (e.g., Heinrich events) (Rühlemann et al., 1999; Vidal et al., 1999; Schmidt et al., 2004; Weldeab et al., 2006; Ziegler et al., 2008). Similar mechanisms for different timescales may be involved and may help to explain ITCZ migration in the past. We propose that North Atlantic variability interacted with the ITCZ position over the MPT.

5.3 Links between the ITCZ location and climate changes associated with the MPT

One of the possible interpretations for the low SSS estimates during interglacial stages spanning the last 450 kyr is a northward shift of the ITCZ. The comparison between the δ^{18}O records of core MD03-2628 and core DSDP 502 suggests that ITCZ migration influenced the Caribbean Sea overall (Figs. 1a and 8b). By contrast, the δ^{18}O record of core ODP 847 obtained from the Eastern Equatorial Pacific Ocean did not record lower δ^{18}O values during interglacials spanning the last 450 kyr (Fig. 8b). Under modern conditions, core ODP 847 is at the southernmost limit of the ITCZ influence (Fig. 1a);

CPD
6, 1229–1265, 2010

therefore, a northward ITCZ migration would not influence the core ODP 847 site.

One way to explain the northward ITCZ migration is a change in the interhemispheric temperature gradient that may be related to an increased northward oceanic heat transfer during interglacials of the past 450 kyr (Trenberth and Caron, 2001). Evidence of enhanced oceanic mass transport can be found in results obtained from the South Atlantic (Peeters et al., 2004). Faunal assemblages in the Cape Basin were used to reconstruct the so-called "Agulhas leakage" (AL), an index for heat and salt export from the Indian Ocean into the Atlantic Ocean. The temporal evolution of this index clearly shows a marked variability with 100 kyr-cycles with enhanced export of warm and salty waters into the South Atlantic during the past five glacial Terminations (Peeters et al., 2004). The strong relationship between the efficiency of the AL and the strength of the AMOC is supported by observations in the modern ocean and by model simulations (Knorr and Lohmann, 2003; Biastoch et al., 2008). The intensity of the AL depends on the location of Southern Ocean oceanographic fronts (SOF) and the related Southern Hemisphere westerlies (Rouault et al., 2009; Biastoch et al., 2009). A poleward migration of the SOF induces changes in wind stress that cause the resumption of the Agulhas currrent and, as a consequence, intense leakage from the Indian Ocean to the Atlantic Basin. At glacial-interglacial timescales, influence of the SOF migration on the AL and its impacts on the AMOC has been invoked for extreme glacial stages (Bard and Rickaby, 2009). On a longer timescale, a study based on past SST from the South Atlantic spanning the MPT has pointed to a shift toward higher SST values during interglacial stages for the last 450 kyr, as compared to older interglacial stages (Becquey and Gersonde, 2002, Fig. 8c). The abrupt change in SST values reflects a southernmost SOF location, implying a stronger AL for the last five interglacial stages as compared to interglacials older than 650 kyr (Becquey and Gersonde, 2002, Fig. 8c). These long-term changes in the SOF location may have induced a more vigorous AMOC during interglacial stages of the last 450 kyr. An enhanced northward oceanic transfer during the interglacial stages could have promoted more intense heat transport to high latitudes, and therefore, warming of the Northern Hemisphere (Chi-

CPD
6, 1229–1265, 2010

ang et al., 2003; Braconnot et al., 2007; Toggweiler, 2009). As a result, the ITCZ could have moved northward. Finally, the combination of a northernmost ITCZ location and an increase in oceanic heat transfer may be involved in the amplification of climate cycles during the last 450 kyr (Fig. 8d).

The final mechanisms to explore are processes that have induced long-term migration of the SOF during the MPT. Model simulations have shown links between the location of the SOF and atmospheric CO_2 through oceanic carbon pump efficiency (Saenko et al., 2005; Toggweiler et al., 2006; Toggweiler and Russell, 2008; Köhler and Bintanja, 2008). The recent record of atmospheric CO_2 from the EPICA spanning the last 800 kyr clearly shows a difference in the glacial-interglacial amplitude for CO_2 changes between the last five climate cycles and for periods older than 450 kyr (Luthi et al., 2008, Fig. 8d). Profound changes in the carbon cycle may need to be invoked in order to explain the transition of the overall climate system from the 41-kyr to the 100-kyr world.

6 Conclusions

The goal of this study was to evaluate the impact of changes in the climate system following the Mid-Pleistocene Transition (MPT) on the Tropical Atlantic Ocean by evaluating past variations in the hydrologic cycle in the Northern Caribbean Sea. In core MD03-2628, we estimated past sea surface salinities (SSS) using reconstructions of the past changes of seawater δ^{18}O relative to modern conditions ($\Delta\delta^{18}$O). The δ^{18}O of seawater was obtained by combining the alkenone sea-surface temperature record with the δ^{18}O of *G. ruber* and by applying a correction for the ice-sheet volume effect over the last 940 kyr. Today, the main control on SSS at the core site is the modern seasonnal Inter-Tropical Convergence Zone (ITCZ) migration. Variations in the $\Delta\delta^{18}$O display a pattern of lower and higher SSS during interglacial and glacial stages, respectively, over the past 940 kyr. Glacial stage values for $\Delta\delta^{18}$O are nearly constant for the last 940 kyr, whereas interglacial values for the 940–650 kyr time-period are

CPD
6, 1229–1265, 2010

higher than for the 450–0 kyr interval.

The core MD03-2628 $\Delta\delta^{18}O$ record allowed us to document the relationships between the low latitude hydrologic cycle and the Atlantic Meridional Overturning Circulation (AMOC) at the glacial/interglacial timescale over the last 940 kyr. We propose that for all glacial periods during the last 940 kyr, the southward position of the ITCZ induced an increase in SSS at the studied site, in association with a reduced AMOC, keeping warm and salty waters at low latitudes, as previously suggested for the last glacial period. On a longer timescale, the $\Delta\delta^{18}O$ results highlight the response of tropical areas to climate changes associated with the MPT. A shift in the $\Delta\delta^{18}O$ values reflects the northward migration of the ITCZ during the last five interglacial periods, when compared to the time-period before 650 kyr. Northward movement during interglacial stages could have been associated with an enhanced cross-equatorial oceanic transport, as supported by evidence from the South Atlantic. The combination of enhanced northward atmospheric and oceanic transfers could have participated in the amplification of climate cycles during the last 450 kyr.

Acknowledgements. Paleoclimate work at CEREGE is supported by grants from the CNRS, the ANR-PICC, the Gary Comer Foundation for Science and Education, the European Community (Project Past4Future) and the Collège de France. We are grateful to Corinne Sonzogni for technical assistance.

The publication of this article is financed by CNRS-INSU.

CPD

6, 1229–1265, 2010

References

Bard, E. and Rickaby, R. E. M.: Migration of the subtropical front as a modulator of glacial climate, Nature, 460, 380–393, 2009.

Becquey, S. and Gersonde, R.: Past hydrographic and climatic changes in the Subantarctic Zone of the South Atlantic – the pleistocene record from ODP Site 1090, Palaeogeogr. Palaeocl., 182, 221–239, 2002.

Bemis, B. E., Spero, H. J., Bijma, J., and Lea, D. W.: Reevaluation of the oxygen isotopic composition of planktonic *foraminifera*: experimental results and revised paleotemperature equations, Paleoceanography, 13, 150–160, 1998.

Berger, A., Li, S., and Loutre, M.-F.: Modelling Northern Hemisphere ice volume over the last 3 Ma, Quaternary Sci. Rev., 18, 1–11, 1999.

Biastoch, A., Boning, C. W., and Lutjeharms, J. R. E.: Agulhas leakage dynamics affects decadal variability in Atlantic overturning circulation, Nature, 456, 489–492, 2008.

Biastoch, A., Boning, C. W., Schwarzkopf, F. U., and Lutjeharms, J. R. E.: Increase in Agulhas leakage due to poleward shift of Southern Hemisphere westerlies, Nature, 462, 495-U188, 2009.

Bintanja, R. and van de Wal, R. S. W.: North American ice-sheet dynamics and the onset of 100 000-yr glacial cycles, Nature, 454, 869–872, 2008.

Braconnot, P., Otto-Bliesner, B., Harrison, S., Joussaume, S., Peterchmitt, J.-Y., Abe-Ouchi, A., Crucifix, M., Driesschaert, E., Fichefet, Th., Hewitt, C. D., Kageyama, M., Kitoh, A., Loutre, M.-F., Marti, O., Merkel, U., Ramstein, G., Valdes, P., Weber, L., Yu, Y., and Zhao, Y.: Results of PMIP2 coupled simulations of the Mid-Holocene and Last Glacial Maximum – Part 2: feedbacks with emphasis on the location of the ITCZ and mid- and high latitudes heat budget, Clim. Past, 3, 279–296, doi:10.5194/cp-3-279-2007, 2007.

Broccoli, A. J., Dahl, K. A., and Stouffer, R. J.: Response of the ITCZ to Northern Hemisphere cooling, Geophys. Res. Lett., 33, L01702, 2006.

Broecker, W. S., Bond, G., Klas, M., Bonani, G., and Wolfli, W. A.: A salt oscillator in the glacial Atlantic? 1. The concept, Paleoceanography, 5, 469–477, 1990.

Chérubin, L. M. and Richardson, P. L.: Caribbean current variability and the influence of the Amazon and Orinoco freshwater plumes, Deep-Sea Res. Pt. I, 54, 1451–1473, 2007.

Chiang, J. C. H., Kushnir, Y., and Giannini, A.: Deconstructing Atlantic intertropical convergence zone variability: influence of the local cross-equatorial sea surface temperature gradient and

remote forcing from the Eastern Equatorial Pacific, J. Geophys. Res.-Atmos., 107(D1-D2), 4004, 2002.
Chiang, J. C. H., Biasutti, M., and Battisti, D. S.: Sensitivity of the Atlantic intertropical convergence zone to last glacial maximum boundary conditions, Paleoceanography, 18, 1094, 2003.
Clark, P. U. and Pollard, D.: Origin of the middle pleistocene transition by ice sheet erosion of regolith, Paleoceanography, 13, 1–9, 1998.
Clark, P. U., Archer, D., Pollard, D., Blum, J. D., Rial, J. A., Brovkin, V., Mix, A. C., Pisias, N. G., and Roy, M.: The middle pleistocene transition: characteristics. mechanisms, and implications for long-term changes in atmospheric $p\mathrm{CO}_2$, Quaternary Sci. Rev., 25, 3150–3184, 2006.
Conte, M. H., Sicre, M. A., Rühlemann, C., Weber, J. C., Schulte, S., Schulz-Bull, D., and Blanz, T.: Global temperature calibration of the alkenone unsaturation index ($U_37^{K'}$) in surface waters and comparison with surface sediments, Geochem. Geophy. Geosy., 7, Q02005, 2006.
Crowley, T. J.: North Atlantic deep water cools the Southern Hemisphere, Paleoceanography, 7, 489–497, 1992.
Dahl, K., Broccoli, A., and Stouffer, R.: Assessing the role of North Atlantic freshwater forcing in millennial scale climate variability: a Tropical Atlantic perspective, Clim. Dynam., 24, 325–346, 2005.
da Silva, A., Young, A. C., and Levitus, S.: Atlas of Surface Marine Data 1994, Volume 1: Algorithms and Procedures, NOAA Atlas NESDIS, 6, US Department of Commerce, Washington, D.C., http://iridl.ldeo.columbia.edu/SOURCES/.DASILVA/, last access: 2008, 1994.
de Garidel-Thoron, T.: Paleoceanography records, Early Pleistocene, Encyclopedia of Quaternary Science, Elsevier, Amsterdam, 1785–1793, 2007.
Dürkoop, A., Hale, W., Mulitza, S., Patzold, J., and Wefer, G.: Late quaternary variations of sea surface salinity and temperature in the Western Tropical Atlantic: evidence from δ^{18}O of *Globigerinoides sacculifer*, Paleoceanography, 12, 764–772, 1997.
Farrell, J. W., Murray, D. W., McKenna, V. S., and Ravelo, A. C.: Upper ocean temperature and nutrient contrasts inferred from Pleistocene planktonic foraminifer δ^{18}O and δ^{13}C in the Eastern Equatorial Pacific, Proceedings of ODP, Sci. Res., 138, 289–319, 1995.
Fratantoni, D. M., Zantopp, R. J., Johns, W. E., and Miller, J. L.: Updated bathymetry of the Anegada-Jungfern Passage complex and implications for Atlantic inflow to the abyssal

Caribbean Sea, J. Mar. Res., 55, 847–860, 1997.
Gordon, A. L.: Oceanography – communication between oceans, Nature, 382, 399–400, 1996.
Hastings, D. W., Russell, A. D., and Emerson, S. R.: Foraminiferal magnesium in *Globerigi-noides sacculifer* as a paleotemperature proxy, Paleoceanography, 13, 161–169, 1998.
Haug, G. H. and Tiedemann, R.: Effect of the formation of the Isthmus of Panama on Atlantic Ocean thermohaline circulation, Nature, 393, 673–676, 1998.
Haug, G. H., Tiedemann, R., Zahn, R., and Ravelo, A. C.: Role of Panama uplift on oceanic freshwater balance, Geology, 29, 207–210, 2001.
Haug, G. H., Gunther, D., Peterson, L. C., Sigman, D. M., Hughen, K. A., and Aeschlimann, B.: Climate and the collapse of Maya civilization, Science, 299, 1731–1735, 2003.
Head, M. J. and Gibbard, P. L.: Early-Middle Pleistocene transitions: an overview and recommendation for the defining boundary, in: Early-Middle Pleistocene Transitions: The Land-Ocean Evidence, edited by: Head, M. J. and Gibbard, P. L., Geological Society of London, Special Publications, London, UK, 247, 1–8, 2005.
Hellweger, F. L. and Gordon, A. L.: Tracing Amazon River water into the Caribbean Sea, J. Mar. Res., 60, 537–549, 2002.
Hernandez-Guerra, A. and Joyce, T. M.: Water masses and circulation in the surface layers of the Caribbean at 66° W, Geophys. Res. Lett., 27, 3497–3500, 2000.
Hoogakker, B. A. A., Rohling, E. J., Palmer, M. R., Tyrrell, T., and Rothwell, R. G.: Underlying causes for long-term global ocean δ^{13}C fluctuations over the last 1.20 Myr, Earth Planet. Sc. Lett., 248, 15–29, 2006.
Hu, C. M., Montgomery, E. T., Schmitt, R. W., and Müller-Karger, F. E.: The dispersal of the Amazon and Orinoco River water in the Tropical Atlantic and Caribbean Sea: observation from space and S-PALACE floats, Deep-Sea Res. Pt. II, 51, 1151–1171, 2004.
Hüls, M. and Zahn, R.: Millennial-scale sea surface temperature variability in the Western Tropical North Atlantic from planktonic foraminiferal census counts, Paleoceanography, 15, 659–678, 2000.
Kameo, K., Shearer, M. C., Droxler, A. W., Mita, I., Watanabe, R., and Sato, T.: Glacial-interglacial surface water variations in the Caribbean Sea during the last 300 ky based on calcareous nannofossil analysis, Palaeogeogr. Palaeocl., 212, 65–76, 2004.
Köhler, P. and Bintanja, R.: The carbon cycle during the Mid Pleistocene Transition: the Southern Ocean Decoupling Hypothesis, Clim. Past, 4, 311–332, doi:10.5194/cp-4-311-2008, 2008.

CPD
6, 1229–1265, 2010

Knorr, G. and Lohmann, G.: Southern ocean origin for the resumption of Atlantic thermohaline circulation during deglaciation, Nature, 424, 532–536, 2003.
Levitus, S. and Boyer, T.: World Ocean Atlas 1994, US Department of Commerce, Washington DC, http://ingrid.ldeo.columbia.edu/SOURCES/.LEVITUS/, last access: 2008, 1994.
Lisiecki, L. E. and Raymo, M. E.: A pliocene-pleistocene stack of 57 globally distributed benthic δ^{18}O record, Paleoceanography, 20, PA1003, 2005.
Liu, Z., Cleaveland, L. C., and Herbert, T. H.: Early onset of 100-kyr cycles in pleistocene tropical SST records, Earth Planet. Sci. Lett., 265, 703–715, 2008.
Luthi, D., Le Floch, M., Bereiter, B., Blunier, T., Barnola, J. M., Siegenthaler, U., Raynaud, D., Jouzel, J., Fischer, H., Kawamura, K., and Stocker, T. F.: High-resolution carbon dioxide concentration record 650 000–800 000 yr before present, Nature, 453, 379–382, 2008.
Martinez, J. I., Mora, G., and Barrows, T. T.: Paleoceanographic conditions in the Western Caribbean Sea for the last 560 kyr as inferred from planktonic *foraminifera*, Mar. Micropaleontol., 64, 177–188, 2007.
Maslin, M. A. and Ridgwell, A. J.: Mid-pleistocene revolution and the “eccentricity myth”, in: Early-Middle Pleistocene Transitions: The Land-Ocean Evidence, edited by: Head, M. J. and Gibbard, P. L., Geological Society of London, Special Publications, London, UK, 247, 19–34, 2005.
McClymont, E. L. and Rosell-Mele, A.: Links between the onset of modern walker circulation and the mid-Pleistocene climate transition, Geology, 33, 389–392, 2005.
McClymont, E. L., Rosell-Mele, A., Haug, G. H. and Lloyd, J. M.: Expansion of subarctic water masses in the North Atlantic and Pacific oceans and implications for mid-pleistocene ice sheet growth, Paleoceanography, 23, PA4214, 2008.
Mix, A. C., Ruddiman, W. F., and McIntyre, A.: Late Quaternary paleoceanography of the Tropical Atlantic, I. Spatial variability of annual mean sea-surface temperatures 0–20 000 yr BP, Paleoceanography, 1, 43–66, 1986.
Morrison, J. M. and Nowlin, W. D.: General distribution of water masses within the Eastern Caribbean Sea during the winter of 1972 and fall of 1973, J. Geophys. Res.-Oc. Atm., 87, 4207–4229, 1982.
Mulitza, S., Boltovskoy, D., Donner, B., Meggers, H., Paul, A., and Wefer, G.: Temperature: delta O-18 relationships of planktonic foraminifera collected from surface waters, Palaeogeogr. Palaeocl., 202, 143–152, 2003.
Müller-Karger, F. E., McClain, C. R., and Richardson, P. L.: The dispersal of the Amazons water,

Nature, 333, 56–59, 1988.
Paillard, D., Labeyrie, L., and Yiou, P.: Macintosh program performs time-series analysis, EOS. Trans. AGU, 77, 379, 1996.
Peeters, F. J. C., Acheson, R., Brummer, G. J. A., de Ruijter, W. P. M., Schneider, R. R., Ganssen, G. M., Ufkes, E., and Kroon, D.: Vigorous exchange between the Indian and Atlantic oceans at the end of the past five glacial periods, Nature, 430, 661–665, 2004.
Prell, W. L.: Oxygen and carbon isotope stratigraphy for the quaternary of hole 502B: evidence for two modes of isotopic variability, Init. Rep. DSDP, 68, 455–464, 1982.
Rahmstorf, S.: The thermohaline ocean circulation: a system with dangerous thresholds? An editorial comment, Clim. Change, 46, 247–256, 2000.
Rahmstorf, S.: Ocean circulation and climate during the past 120 000 yr, Nature, 419, 207–214, 2002.
Rahmstorf, S., Crucifix, M., Ganopolski, A., Goosse, H., Kamenkovich, I., Knutti, R., Lohmann, G., Marsh, R., Mysak, L. A., Wang, Z. M., and Weaver, A. J.: Thermohaline circulation hysteresis: a model intercomparison, Geophys. Res. Lett., 32, L23605, 2005.
Rahmstorf, S.: Thermohaline ocean circulation, in: Encyclopedia of Quaternary Sciences, edited by: Elias, S. A., Elsevier, Amsterdam, 2006.
Raymo, M. E., Oppo, D. W., and Curry, W.: The mid-Pleistocene climate transition: a deep sea carbon isotopic perspective, Paleoceanography, 12, 546–559, 1997.
Raymo, M. E., Lisiecki, L. E., and Nisancioglu, K. H.: Plio-Pleistocene ice volume, Antarctic climate, and the global δ^{18}O record, Science, 313, 492–495, 2006.
Raymo, M. E. and Huybers, P.: Unlocking the mysteries of the ice ages, Nature, 451, 284–285, 2008.
Regenberg, M., Steph, S., Nurnberg, D., Tiedemann, R., and Garbe-Schonberg, D.: Calibrating Mg/Ca ratios of multiple planktonic foraminiferal species with δ^{18}O-calcification temperatures: paleothermometry for the upper water column, Earth Planet. Sc. Lett., 278, 324–336, 2009.
Reijmer, J. J. G. and Andresen, N.: Mineralogy and grain size variations along two carbonate margin-to-basin transects (Pedro Bank, Northern Nicaragua Rise), Sediment. Geol., 198, 327–350, 2007.
Rosell-Mele, A., Bard, E., Emeis, K. C., Grimalt, J. O., Muller, P., Schneider, R., Bouloubassi, I., Epstein, B., Fahl, K., Fluegge, A., Freeman, K., Goni, M., Guntner, U., Hartz, D., Hellebust, S., Herbert, T., Ikehara, M., Ishiwatari, R., Kawamura, K., Kenig, F., de Leeuw, J., Lehman, S.,

CPD
6, 1229–1265, 2010

Sea-surface salinity changes in the Caribbean Sea

S. Sepulcre et al.

Mejanelle, L., Ohkouchi, N., Pancost, R. D., Pelejero, C., Prahl, F., Quinn, J., Rontani, J. F., Rostek, F., Rullkotter, J., Sachs, J., Blanz, T., Sawada, K., Schutz-Bull, D., Sikes, E., Sonzogni, C., Ternois, Y., Versteegh, G., Volkman, J. K., and Wakeham, S.: Precision of the current methods to measure the alkenone proxy $U_{37}^{K'}$ and absolute alkenone abundance in sediments: Results of an interlaboratory comparison study, Geochem. Geophy. Geosy., 2, 2000GC000141, 2001.

Rouault, M., Penven, P., and Pohl, B.: Warming in the Agulhas Current system since the 1980's, Geophys. Res. Lett., 36, L12602, 2009.

Rühlemann, C., Mulitza, S., Muller, P. J., Wefer, G., and Zahn, R.: Warming of the Tropical Atlantic Ocean and slowdown of thermohaline circulation during the last deglaciation, Nature, 402, 511–514, 1999.

Rühlemann, C., Mulitza, S., Lohmann, G., Paul, A., Prange, M., and Wefer, G.: Intermediate depth warming in the Tropical Atlantic related to weakened thermohaline circulation: combining paleoclimate data and modeling results for the last deglaciation, Paleoceanography, 19, PA1025, 2004.

Rutherford, S. and D'Hondt, S.: Early onset and tropical forcing of 100 000-yr Pleistocene glacial cycles, Nature, 408, 72–75, 2000.

Saenko, O. A., Fyfe, J. C., and England, M. H.: On the response of the oceanic wind-driven circulation to atmospheric CO_2 increase, Clim. Dynam., 25, 415–426, 2005.

Schmidt, G. A., Bigg, G. R., and Rohling, E. J.: Global Seawater Oxygen-18 Database, http://data.giss.nasa.gov/o18data/, last access: 2008, 1999.

Schmidt, M. W., Spero, H. J., and Lea, D. W.: Links between salinity variation in the Caribbean and North Atlantic thermohaline circulation, Nature, 428, 160–163, 2004.

Schmidt, M. W., Vautravers, M. J., and Spero, H. J.: Western Caribbean sea surface temperatures during the late Quaternary, Geochem. Geophy. Geosy., 7, Q02P10, 2006.

Schmieder, F., von Dobeneck, T., and Bleil, U.: The mid-pleistocene climate transition as documented in the deep South Atlantic Ocean: initiation, interim state and terminal event, Earth Planet. Sc. Lett., 179, 539–549, 2000.

Schmitz, W. J. and Richardson, P. L.: On the sources of the Florida current, Deep-Sea Res., 38(suppl.), 379–409, 1991.

Schmuker, B. and Schiebel, R.: Planktic foraminifers and hydrography of the Eastern and Northern Caribbean Sea, Mar. Micropaleontol., 46, 387–403, 2002.

Schulz, K. G. and Zeebe, R. E.: Pleistocene glacial terminations triggered by synchronous

changes in Southern and Northern Hemisphere insolation: the insolation canon hypothesis, Earth Planet. Sc. Lett., 249, 326–336, 2006.
Sepulcre, S., Tachikawa, K., Vidal, L., Thouveny, N., and Bard, E.: Preservation state of metastable magnesian calcite in periplatform sediment from the Caribbean Sea over the last million years, Geochem. Geophy. Geosy., 10, Q11013, doi:10.1029/2009GC002779, 2009.
Sonzogni, C., Bard, E., Rostek, F., Dollfus, D., Rosell-Mele, A., and Eglinton, G.: Temperature and salinity effects on alkenone ratios measured in surface sediments from the Indian Ocean, Quaternary Res., 47, 344–355, 1997.
Steph, S., Tiedemann, R., Prange, M., Groeneveld, J., Nurnberg, D., Reuning, L., Schulz, M., and Haug, G. H.: Changes in Caribbean surface hydrography during the Pliocene shoaling of the Central American Seaway, Paleoceanography, 21, PA4221, 2006.
Stouffer, R. J., Yin, J., Gregory, J. M., Dixon, K. W., Spelman, M. J., Hurlin, W., Weaver, A. J., Eby, M., Flato, G. M., Hasumi, H., Hu, A., Jungclaus, J. H., Kamenkovich, I. V., Levermann, A., Montoya, M., Murakami, S., Nawrath, S., Oka, A., Peltier, W. R., Robitaille, D. Y., Sokolov, A., Vettoretti, G., and Weber, S. L.: Investigating the causes of the response of the thermohaline circulation to past and future climate changes, J. Climate, 19(8), 1365–1387, 2006.
Taylor, M. A., Enfield, D. B., and Chen, A. A.: Influence of the Tropical Atlantic versus the Tropical Pacific on Caribbean rainfall, J. Geophys. Res.-Oc., 107, 3127, 2002.
Toggweiler, J. R.: Shifting westerlies, Science, 323, 1434–1435, 2009.
Toggweiler, J. R. and Russell, J.: Ocean circulation in a warming climate, Nature, 451, 286–288, 2008.
Toggweiler, J. R., Russell, J. L., and Carson, S. R.: Midlatitude westerlies, atmospheric CO_2, and climate change during the ice ages, Paleoceanography, 21, PA2005, 2006.
Tomczak, M. and Godfrey, J. S: Regional Oceanography: An Introduction, Second Edition, Daya Books, Delhi, 390 pp., 2003.
Trenberth, K. E. and Caron, J. M.: Estimates of meridional atmosphere and ocean heat transports, J. Climate, 14, 3433–3443, 2001.
Tzedakis, P. C., Raynaud, D., McManus, J. F., Berger, A., Brovkin, V., and Kiefer T.: Interglacial diversity, Nat. Geosci., 2, 751–755, 2009.
Tziperman, E. and Gildor, H.: On the mid-pleistocene transition to 100-kyr glacial cycles and the asymmetry between glaciation and deglaciation times, Paleoceanography, 18, 1001, PA2005, 2003.

CPD
6, 1229–1265, 2010

Vidal, L., Schneider, R. R., Marchal, O., Bickert, T., Stocker, T. F., and Wefer, G.: Link between the North and South Atlantic during the Heinrich events of the last glacial period, Clim. Dynam., 15, 909–919, 1999.
Waelbroeck, C., Labeyrie, L., Michel, E., Duplessy, J. C., McManus, J. F., Lambeck, K., Balbon, E., and Labracherie, M.: Sea-level and deep water temperature changes derived from benthic foraminifera isotopic records, Quaternary Sci. Rev., 21, 295–305, 2002.
Waelbroeck, C., Mulitza, S., Spero, H., Dokken, T., Kiefer, T., and Cortijo, E.: A global compilation of late Holocene planktonic foraminiferal $\delta^{18}O$: relationship between surface water temperature and $\delta^{18}O$, Quaternary Sci. Rev., 24, 853–868, 2005.
Wan, X., Chang, P., and Schmidt, M. W.: Causes of Tropical Atlantic paleosalinity variation during periods of reduced AMOC, Geophys. Res. Lett., 37, L04603, doi:10.1029/2009GL042013, 2010.
Wang, C. Z. and Lee, S. K.: Atlantic warm pool, Caribbean low-level jet, and their potential impact on Atlantic hurricanes, Geophys. Res. Lett., 34(2), L02703, doi:10.1029/2007GL031149, 2007.
Watanabe, T., Winter, A., and Oba, T.: Seasonal changes in sea surface temperature and salinity during the Little Ice Age in the Caribbean Sea deduced from Mg/Ca and $^{18}O/^{16}O$ ratios in corals, Mar. Geol., 173, 21–35, 2001.
Weldeab, S., Schneider, R. R., and Kolling, M.: Deglacial sea surface temperature and salinity increase in the Western Tropical Atlantic in synchrony with high latitude climate instabilities, Earth Planet. Sc. Lett., 241, 699–706, 2006.
Wolff, T., Mulitza, S., Arz, H., Patzold, J., and Wefer, G.: Oxygen isotopes versus CLIMAP (18 ka) temperatures: a comparison from the Tropical Atlantic, Geology, 26, 675–678, 1998.
Wüst, G.: Stratification and Circulation in the Antillean-Caribbean Basins, Columbia University Press, New York, 1964.
Yin, Q. Z. and Berger A.: Insolation and CO_2 contribution to the interglacial climate before and after the mid-brunhes event, Nat. Geosci., 3, 243–246, 2010.
Zaucker, F. and Broecker, W. S.: The influence of atmospheric moisture transport on the fresh water balance of the Atlantic drainage basin: general circulation model simulations and observations, J. Geophys. Res., 97, 2765–2773, 1992.
Ziegler, M., Nurnberg, D., Karas, C., Tiedemann, R., and Lourens, L. J.: Persistent summer expansion of the Atlantic warm pool during glacial abrupt cold events, Nat. Geosci., 1, 601–605, 2008.

CPD
6, 1229–1265, 2010

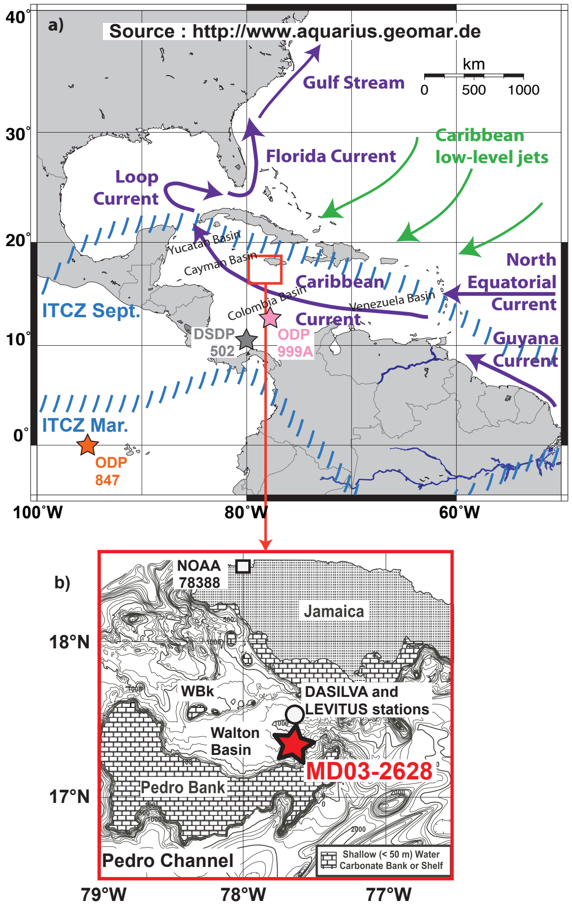

Fig. 1. The modern setting of the studied zone and the location of core MD03-2628. **(a)** The climatic and oceanic context of the Caribbean Sea: purple arrows are surface currents; green arrows are winds; and blue hatched zones are the seasonal extreme positions of the Inter-Tropical Convergence Zone (ITCZ, e.g., Haug et al., 2003). The locations of cores ODP 999A (12°45′ N, 78°44′ W, 2827 m of water depth, pink star); DSDP 502 (11° N, 80° W, 3051 m of water depth, gray star); and ODP 847 (0° N, 95° W, 3373 m of water depth, orange star) are also specified. **(b)** A zoom-in of the Walton Basin and the location of core MD03-2628 (WBk: Walton Bank). The location of the LEVITUS (1994) and the DASILVA (da Silva et al., 1994) stations at 17.5° N, 77,5° W; and of the NOAA (station 78388) station (18.47° N, 77.99° W) are also specified in Fig. 1b (adapted from Reijmer and Andresen, 2007).

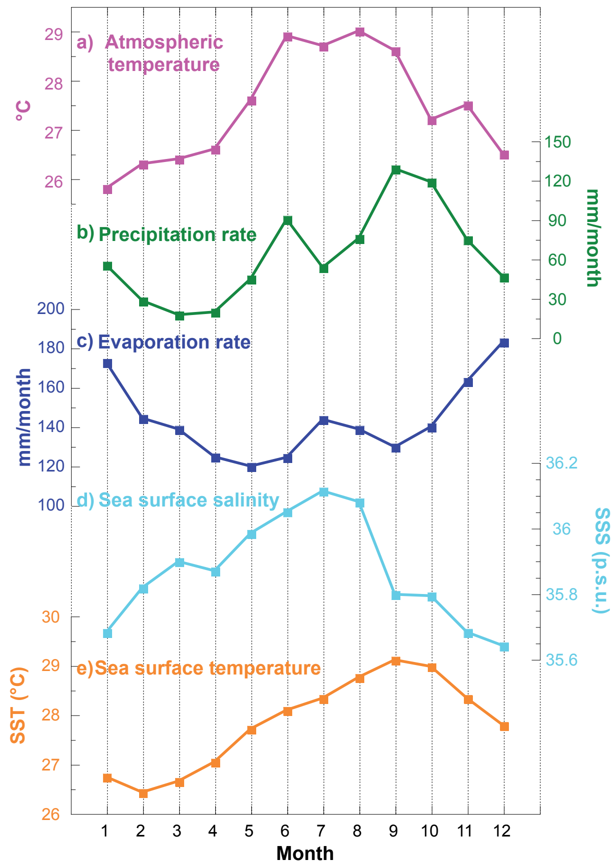

Fig. 2. Monthly climate and sea-surface water parameters. **(a)** Atmospheric temperature from NOAA climate station 78388; **(b)** precipitation; **(c)** evaporation rates from the DASILVA dataset (da Silva et al., 1994); **(d)** Sea-surface salinity (SSS); and **(e)** temperature (SST) from the LEVITUS (1994) dataset.

CPD
6, 1229–1265, 2010

Sea-surface salinity changes in the Caribbean Sea

S. Sepulcre et al.

CPD

6, 1229–1265, 2010

Sea-surface salinity changes in the Caribbean Sea

S. Sepulcre et al.

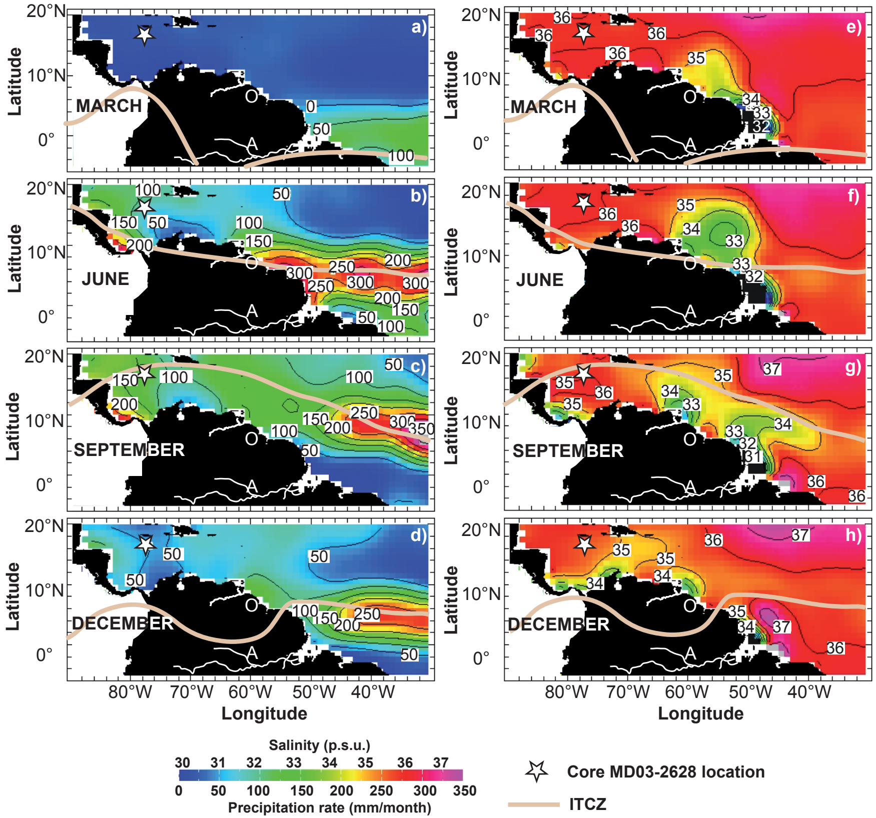

Fig. 3. Maps of precipitation rates **(a–d)** and sea surface salinities **(e–h)** during March (a and e), June (b and f), September (**c** and g), and December (d and h). The core MD03-2628 location is shown by a star and the ITCZ position is shown by the thick beige line (e.g., Haug et al., 2003). The Orinoco and Amazon Rivers are designed by the O and A letters, respectively. Maps were constructed from http://ingrid.ldeo.columbia.edu/ using the DASILVA (da Silva et al., 1994) and LEVITUS (1994) datasets.

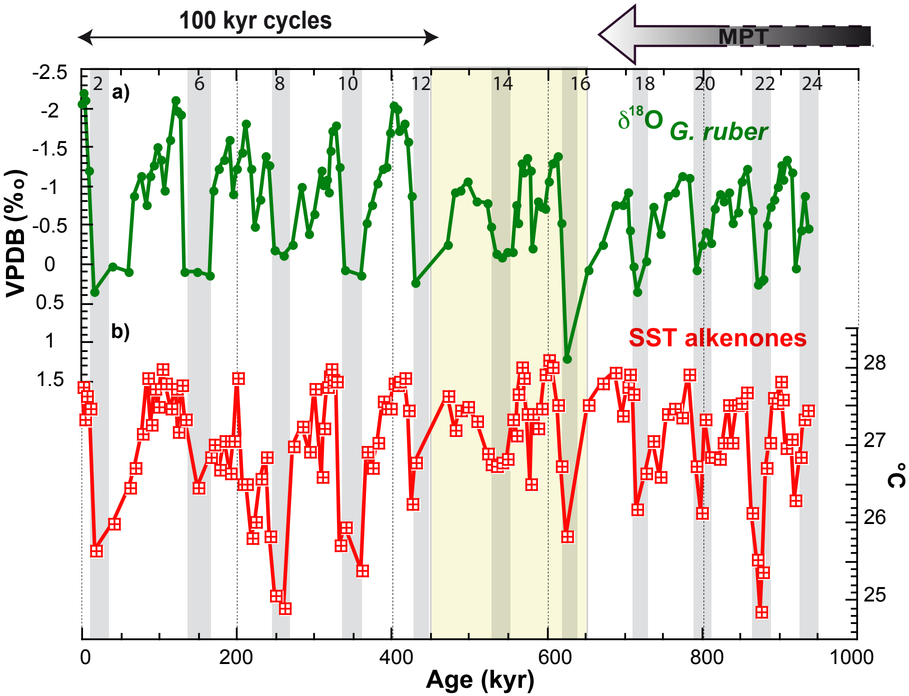

Fig. 4. Core MD03-2628 records for: **(a)** the δ^{18}O of the planktonic *foraminifera Globigerinoides ruber* (green curve and dots); and **(b)** sea-surface temperatures (red curve and squares) as determined by the $U^{K'}_{37}$ index. Light gray bars and even numbers show the glacial stages as defined by δ^{18}O. The yellow area indicates the 650 to 450 kyr time interval when the duration and shape of the climate cycles changed (see text and Fig. 5 for details).

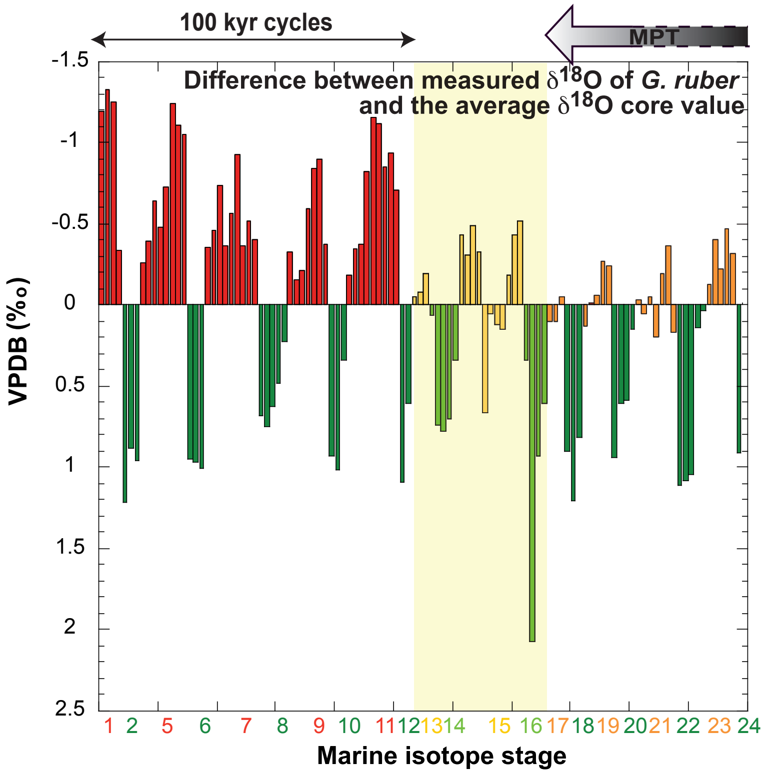

Fig. 5. The difference between the measured $\delta^{18}O$ of *G. ruber* and the average core MD03-2628 $\delta^{18}O$ value (−0.8‰) used to illustrate the nearly constant values for glacial stages (green bars) and the change in the $\delta^{18}O$ value for interglacial stages between the end of the MPT (from 650 kyr down core, orange bars) and the last 450 kyr (red bars). The yellow area indicates the 650 to 450 kyr time interval when the duration and shape of the climate cycles changed (yellow and light green bars for interglacial and glacial stages, respectively).

CPD
6, 1229–1265, 2010

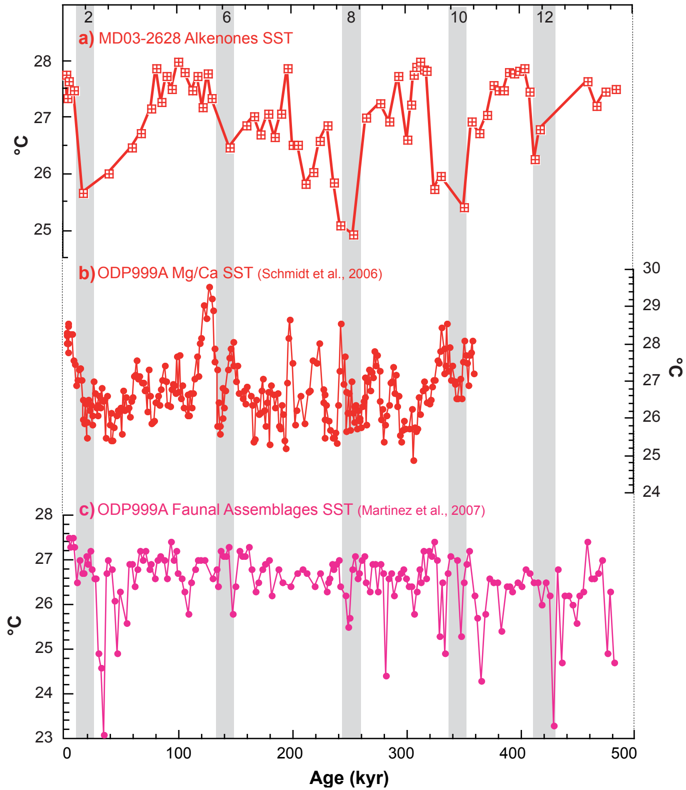

Fig. 6. A comparison of the MD03-2628 sea-surface temperature (SST) record with other SST reconstructions in the Caribbean Sea. **(a)** A zoom-in for the last 500 kyr for the SST results obtained using the $U_{37}^{K'}$ index on core MD03-2628; **(b)** and **(c)** results obtained on ODP core 999A (Fig. 1a) by (b) Schmidt et al. (2004, 2006), with Mg/Ca SST results (red curve and dots) and by (c) Martinez et al. (2007); with mean annual values of faunal SST reconstructions (pink curve and dots). Light gray bars and even numbers are the same as in Fig. 4.

CPD
6, 1229–1265, 2010

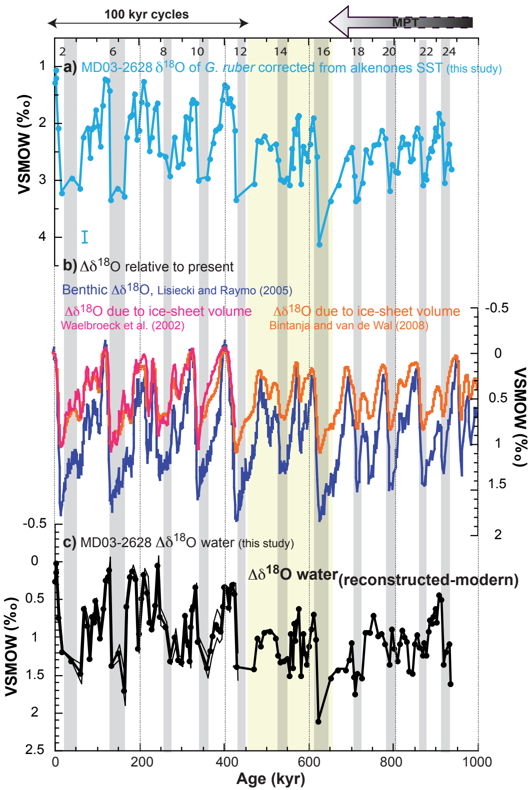

Fig. 7. The calculation steps for the correction procedure for MD03-2628 δ^{18}O for *Globigerinoides ruber*. **(a)** The core MD03-2628 δ^{18}O record (blue curve and dots) corrected for temperature effects using sea-surface temperatures (from the $U^{K'}_{37}$ index) and the equation of Mulitza et al. (2003). The error bar at the left shows the error in the calculation due to SST uncertainty. **(b)** The global oceanic $\Delta\delta^{18}$O relative to the present; the global benthic $\Delta\delta^{18}$O stack from Lisiecki and Raymo (2005) is shown in dark blue. From this record, Bintanja and van de Wal (2008) extracted the ice-volume effect (IVE, orange curve) in global $\Delta\delta^{18}$O. The IVE effect was also recontructed by Waelbroeck et al. (2002) (pink curve). See the text for calculation details. **(c)** Variations in the δ^{18}O of seawater relative to modern values (noticed $\Delta\delta^{18}$O) at the core MD03-2628 location calculated using the records in (a) and (b). The black bold line is the average of both of the IVE corrections from Waelbroeck et al. (2002) and Bintanja and van de Wal (2008). The standard deviation is indicated by the thin lines. Light gray bars, even numbers, and yellow areas in (a) and (c) are the same as in Fig. 4.

CPD

6, 1229–1265, 2010

Sea-surface salinity changes in the Caribbean Sea

S. Sepulcre et al.

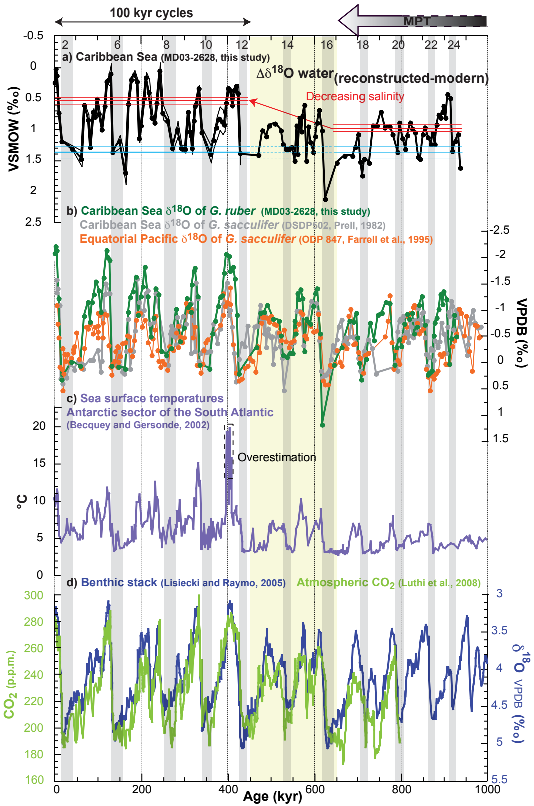

Fig. 8. **(a)** Mean variations for the δ^{18}O of seawater relative to modern values (the noticed $\Delta\delta^{18}$O) at the core MD03-2628 location as a proxy for past sea-surface salinities (SSS). The light blue bold line represents the average glacial values for the 950–650 and the 450–0 kyr time interval. The thin lines are the error at $1\sigma_m$. The red bold lines represent, for each time interval (950–650 and 450–0 kyr), the associated mean $\Delta\delta^{18}$O value for interglacial stages (thin red lines exhibit the error given by $1\sigma_m$). The red arrow indicates the shift in past-SSS values for interglacial stages occuring after 650 kyr. **(b)** A comparison between the planktonic δ^{18}O records of core MD03-2628 (green curve and dots, this study) with the δ^{18}O of *G. sacculifer* records from the Southern Caribbean Sea (DSDP 502, Fig. 1a, Prell, 1982, gray curve and dots) and the Equatorial Pacific (ODP 847, Fig. 1a, Farell et al., 1995, orange curve and dots). **(c)** The sea-surface temperature record from the Antarctic sector of the South Atlantic (core ODP 1090, Becquey and Gersonde, 2002). **(d)** The global benthic δ^{18}O record from Lisiecki and Raymo (2005) in dark blue, and past atmospheric CO_2 concentrations in light green (Luthi et al., 2008). Light gray bars, even numbers, and yellow areas in (a) and (c) are the same as in Fig. 4.